Am J Physiol Heart Circ Physiol 289: H2526–H2535, 2005.
First published August 12, 2005; doi:10.1152/ajpheart.00658.2004.

Mechanical properties of the interaction between fibronectin and $\alpha_5\beta_1$-integrin on vascular smooth muscle cells studied using atomic force microscopy

Zhe Sun,[1] Luis A. Martinez-Lemus,[1] Andreea Trache,[1] Jerome P. Trzeciakowski,[2] George E. Davis,[3] Ulrich Pohl,[4] and Gerald A. Meininger[1]

[1]*Department of Medical Physiology,* [2]*Department of Pharmacology and Toxicology, and* [3]*Department of Pathology and Laboratory Medicine, Cardiovascular Research Institute-Division of Vascular Biology, Texas A&M University System Health Science Center, College Station, Texas; and* [4]*Institute of Physiology, Ludwig Maximilians University, Munich, Germany*

Submitted 2 July 2004; accepted in final form 4 August 2005

Sun, Zhe, Luis A. Martinez-Lemus, Andreea Trache, Jerome P. Trzeciakowski, George E. Davis, Ulrich Pohl, and Gerald A. Meininger. Mechanical properties of the interaction between fibronectin and $\alpha_5\beta_1$-integrin on vascular smooth muscle cells studied using atomic force microscopy. *Am J Physiol Heart Circ Physiol* 289: H2526–H2535, 2005. First published August 12, 2005; doi:10.1152/ajpheart.00658.2004.—The mechanical properties of integrin-extracellular matrix (ECM) interactions are important for the mechanotransduction of vascular smooth muscle cells (VSMC), a process that is associated with focal adhesions, and can be of particular significance in cardiovascular disease. In this study, we characterized the unbinding force and binding activity of the initial fibronectin (FN)-$\alpha_5\beta_1$ interaction on the surface of VSMC using atomic force microscopy (AFM). It is postulated that these initial binding events are important to the subsequent focal adhesion assembly. FN-VSMC adhesions were selectively blocked by antibodies against α_5- and β_1-integrins as well as RGD-containing peptides but not by antibodies against α_4- and β_3-integrins, indicating that FN primarily bound to $\alpha_5\beta_1$. A characteristic unbinding force of 39 ± 8 pN was observed and interpreted to represent the FN-$\alpha_5\beta_1$ single-bond strength. The ability of FN to adhere to VSMC (binding probability) was significantly reduced by integrin antagonists, serum starvation, and platelet-derived growth factor (PDGF)-BB, whereas lysophosphatidic acid (LPA) increased FN binding. However, no significant change in the resolved unbinding force was observed. After engagement, the force required to dislodge the FN-coated bead from VSMC increased with increasing of contact time, suggesting a time-dependent increase in number of adhesions and/or altered binding affinity. LPA enhanced this process, whereas PDGF reduced it, suggesting that these factors also affect the multimolecular process of focal contact assembly. Thus AFM is a powerful tool for the characterization of the mechanical properties of integrin-ECM interactions and their regulation. Our results indicate that the functional activity of $\alpha_5\beta_1$ and focal contact assembly can be rapidly regulated.

bond strength; lysophosphatidic acid; platelet-derived growth factor; mechanical forces; mechanobiology; focal adhesions; focal contacts

MECHANOBIOLOGY is an important field of biology and medicine that deals with how cells sense and respond to mechanical signals from their environment. In the cardiovascular system, mechanical forces play a role in normal function as well as in pathophysiological responses. Understanding the mechanical properties of the molecular and cellular components involved in mechanosensation and transduction is essential to build an understanding of the physical integration that exists between vascular cells and their environment. Integrins, a family of transmembrane heterodimeric receptors, have been proposed to play a crucial role in the mechanical functions of vascular smooth muscle cells (VSMC) as they couple the cytoskeleton with the extracellular matrix (ECM) and support cellular signaling for the regulation of vascular tone (8, 16). Compared with other cell surface receptors, integrins have a relatively low affinity for their binding sites in the ECM (1), and it has been suggested that integrin functional expression and binding affinity can be regulated (10, 23). These characteristics of integrin-ECM interactions may facilitate rapid and dynamic processes such as cell migration, remodeling, and contractile activation in response to mechanical stimuli. The major goal of this study was to characterize the mechanical properties of the fibronectin (FN)-$\alpha_5\beta_1$-integrin interaction in vascular smooth muscle using atomic force microscopy (AFM). A majority of previous studies of integrin function have focused on the intracellular signaling downstream of integrins. By comparison, studies of the mechanical properties of the integrin-ECM interaction are less numerous. A particular goal of this study was to quantify the unbinding force and binding activity between FN and $\alpha_5\beta_1$-integrin on VSMC.

Advances in understanding the mechanical characteristics of integrin-ECM interactions have been limited in part by the lack of appropriate technological approaches that permit accurate measurement and delivery of nano- and picoscale forces to specific receptor-ligand interactions. Laser (7) and magnetic (22) entrapment of ECM-coated beads as well as AFM have been found increasingly useful as tools to study ECM-integrin interactions and cytoskeletal behavior and to measure adhesion forces of different ligand-receptor pairs, including the binding force between integrins and several ECM proteins (2, 13, 19). In the current study, we used AFM to selectively resolve mechanical interactions between FN and $\alpha_5\beta_1$-integrin on VSMC. We also used AFM to assess the regulatory effects of several VSMC-activating factors on the interaction between FN and $\alpha_5\beta_1$-integrin.

MATERIALS AND METHODS

Cell isolation and culture. VSMC were isolated from first-order feed arterioles of rat cremaster muscles using previously described methods (24). Cells were cultured in DMEM/F-12 supplemented with 10% fetal bovine serum (FBS) and used in the experiments at *passages 3–10.*

AFM imaging and force measurement. A Bioscope System (model 3A, Digital Instruments, Santa Barbara, CA) AFM mounted on an

Address for reprint requests and other correspondence: G. A. Meininger, Dalton Cardiovascular Research Center, University of Missouri-Columbia, 134 Research Park Drive, Columbia, MO 65211 (e-mail: Meiningerg@missouri.edu).

The costs of publication of this article were defrayed in part by the payment of page charges. The article must therefore be hereby marked "*advertisement*" in accordance with 18 U.S.C. Section 1734 solely to indicate this fact.

Axiovert 100 TV inverted microscope (Zeiss, Thornwood, NY) was used in contact mode operation to acquire images of cultured VSMC. The AFM probes used were silicon nitride microlevers (model MLCT-AUHW) purchased from Thermomicroscope with a spring constant ranging from 11 to 16 pN/nm. The cantilevers were calibrated using the thermal noise method by Asylum Research (Santa Barbara, CA). This method is subject to an estimated 20% error. Following calibration, we applied a mean value to the spring constant of 14.7 pN/nm to calculate all adhesion forces. To measure the force required to break integrin-ECM bonds, AFM probes were labeled with FN and allowed to repeatedly touch and retract from the surface of VSMC in force mode operation. During AFM probe retraction, if a specific adhesion had occurred, the rupture of this adhesion was detected as a small sharp shift in the deflection curve compared with the smooth curve recorded during the tip approach. With the application of the spring constant of AFM probe cantilever, all deflection shifts in a force curve were detected and quantified using a proprietary software package (NforceR) to determine the adhesion force of integrin-ECM bindings and analyzed using Matlab software (MathWorks, Natick, MA). For each experiment, the same AFM probe was used to obtain data from control and treated cells. The order of sampling was randomized. With each probe, 500–600 force curves were sampled from 10 randomly selected cells (50–60 curves/cell) for each of the control and treated groups. The binding probabilities were determined as (number of force curves with adhesions)/(number of total force curves sampled).

Bioactive coating of AFM tips. The AFM tip-coating method was adapted from Lehenkari and Horton (13). Polyethylene glycol (PEG, Sigma, St. Louis, MO) was used to cross-link human plasma FN (GIBCO-BRL) onto silicon nitride tips. The tip was first incubated with 10 mM PEG for 5 min, washed four times with water, and then incubated with FN (1 mg/ml) for 1 min. The tip was then washed four times with PBS. Spring constants were assumed to be unchanged after protein labeling.

Measurement of mechanical force between an FN-coated bead and VSMC. To assess the mechanical force of the interaction between clustered integrins and FN, silicon nitride cantilevers with a 2-μm bead fused to the tip were used (Novascan, Ames, IA). The bead was first coated with FN. The AFM probes with an FN-coated bead were brought into contact with the cell surface for different periods of contact with the cell (2, 5, and 8 min), the probes were then pulled away from the cell surface in the *z*-axis direction until a rupture point was reached, and the rupture forces were recorded. These experiments were conducted in Hanks' balanced salt saline (HBSS) at room temperature.

Experimental protocols used to determine binding selectivity. To determine the specificity of the integrin-FN bond, experiments were performed on cells incubated for 45 min in cell culture medium in the presence of either an anti-α_5-integrin monoclonal antibody (HMα5–1), an anti-β_1-integrin monoclonal antibody (HMβ1–1), an anti-β_3-integrin monoclonal antibody (F11), or an anti-α_4 rat integrin monoclonal antibody (MRα4–1). Unless otherwise specified, all antibodies were purchased from BD Pharmingen (San Diego, CA) and used at a concentration of 16 μg/ml. Adhesion-force and binding probability were measured under treated and untreated conditions. Another series of blockade experiments were performed after cells were incubated for 45 min at 37°C with either an integrin-binding RGD-containing peptide or an RGE-containing peptide as negative control. These peptides were obtained from GIBCO-BRL and were used at concentrations of 0.8 mM and 0.1 mM.

To determine the effects of VSMC-activating factors on the mechanical characteristics of the integrin-FN bond, cells were incubated in medium without serum for 2 h (short-term serum starvation) or for 20 h (long-term serum starvation) at 37°C, after which the bond adhesion-force and binding probability were determined as described above. Lysophosphatatic acid (LPA, 1 μM), sphingosine-1-phosphate [S1P, 1 μM; produced as previously described (3)], or platelet-derived growth factor (PDGF-BB, 10 and 100 ng/ml) (Sigma) were added to cell culture medium for a 2-h period of treatment either immediately after serum withdrawal or after 18 h of cell culture in serum-free medium.

Integrin identification on the surface of VSMC. As the functional experiments indicated that the FN-integrin bond was mediated by $\alpha_5\beta_1$-integrin, the cell membrane expression of this integrin was determined by flow cytometry for control cells and cells exposed to long- and short-term serum starvation or cells treated with either LPA or PDGF. The spatial localization of this integrin on VSMC was further characterized using confocal microscopy.

FN coating of glass beads mounted on AFM probes and fluorescent polystyrene beads. AFM probes with biotin-labeled glass beads were purchased from Novascan with manufacturer spring constants of 0.06 N/m. FN was first biotinylated using EZ-Link Sulfo-NHS-LC-Biotin (Pierce, Rockford, IL) following instructions provided by the manufacturer. Briefly, 200 μl of FN (1 mg/ml) was mixed with 6 μl of Sulfo-NHS-LC-Biotin (10 mg/ml) in a microcentrifuge tube (Corning, Corning, NY). The mixture was incubated on ice for 2 h and was filtered through a microconcentrator (Millipore, Bedford, MA) to remove the unreacted biotin reagent. The filtered proteins were dissolved in Dulbecco's phosphate-buffered saline (DPBS) with 0.1% NaN_3 (Sigma) at a concentration of ~0.5 mg/ml. AFM probes with biotin-labeled beads were incubated with avidin (1 mg/ml, Sigma) for 5 min at room temperature. The probes were then washed 5 times with DPBS and incubated with biotinylated FN for 5 min at room temperature, followed by five times washing with DPBS.

In an additional series of experiments, fluorescent polystyrene beads were coated with FN and applied on VSMC to verify $\alpha_5\beta_1$ clustering at the bead-cell interface. The fluorescent polystyrene beads (5.5-μm diameter) were purchased from Bangs Laboratory (Fishers, IN) with internal dragon-green fluorescence (480/520 nm excitation/emission) and steptavidin coating. The beads were spun down and washed three times with DPBS. After being washed, beads were incubated with biotin-conjugated FN at room temperature for 30 min on a rolling plate. The beads were then washed three times with DPBS and resuspended in 80 μl DPBS.

Cell staining for flow cytometry. Cells were washed twice with PBS and incubated with versene (GIBCO-BRL, Carlsbad, CA) at 37°C for 10 min. The detached cells were pelleted by centrifugation and suspended and incubated in blocking buffer (HBSS with 1% BSA) on ice for 30 min. Cells were then centrifuged and suspended in 100 μl blocking buffer with primary antibody (HMα5–1, 25 μg/ml) and incubated on ice for 30 min. After the incubation, cells were washed twice with HBSS. Cells were then suspended in 100 μl blocking buffer and incubated with FITC-labeled secondary antibody (1:100 dilution) for another 30 min on ice in dark environment. Cells were washed twice and suspended in 400 μl HBSS. Immediately after suspension, cell fluorescence was measured by flow cytometry.

Cell staining for fluorescence immunocytochemistry and confocal microscopy. Cells were allowed to grow to 50% confluency on glass-bottom tissue culture dishes (35 mm). For experiments with FN-coated fluorescent beads, cells were incubated with FN-coated beads (40 μl of bead-containing solution mixed with 1.5 ml medium/dish) for 2 h at 37°C. Cells were fixed with 2% paraformaldehyde and quenched with glycine buffer (0.1 mM glycine). After being washed, cells were incubated with primary antibodies (1:200 dilution in labeling buffer: 150 mM NaCl, 15 mM $Na_3C_6H_5O_7$, 0.05% Triton X-100, 2% BSA) overnight at 4°C. Cells were washed six times with cold washing buffer (150 mM NaCl, 15 mM $Na_3C_6H_5O_7$, 0.05% Triton X-100), followed by incubation with Cy5-labeled secondary antibody (1:100 dilution in labeling buffer) and Alexa 488-conjugated phalloidin (1:50 dilution) for 1 h at room temperature in a dark environment. The cells were washed again with cold washing buffer and imaged on a confocal microscope using excitation wavelengths of 647 nm and 488 nm, respectively. A through-focus image set was collected for each cell with a *z*-step interval of 0.2 μm. The images

were analyzed using Imaris software (Bitplane AG, Zurich, Switzerland) and ImagePro Plus software (Media Cybernetics, Carlsbad, CA).

Additional instrumentation. For the flow cytometry experiments, a fluorescence-activated cell sorter (FACSCalibur, Becton-Dickinson, San Jose, CA) equipped with an air-cooled argon-ion laser was used. The laser was tuned to 488 nm and operated at 15-mW output. A band-pass 530/30 filter was used for detection of FITC fluorescence. The data acquisition and analyses were performed using CELL Quest software (Becton Dickinson) with a Macintosh G3 computer. For the confocal microscopy experiments, immunofluorescently labeled cells were visualized using a Leica laser confocal microscope system.

Statistical analysis. The collective adhesion force measurements permitted construction of averaged histograms of force-frequency relationships using Matlab software (MathWorks, Natick, MA). Force curves where no rupture event was detected were counted as nonadhesion events. Single-bond strengths were adjusted using probe sensitivity and spring constant as covariates. Differences between means for the effect of a given treatment were determined using ANOVA. All statistical analyses were performed using SAS system software (SAS Institute, Cary, NC). Differences were considered significant at $P \leq 0.05$.

RESULTS

AFM-contact mode imaging and VSMC topography. A contact-mode deflection image of a cultured VSMC revealed large bands of cytoskeletal filaments underlying the cell membrane (Fig. 1). Contact-mode AFM data of VSMC were also used to generate topographic image of the cell surface. These images indicated cell height averaged 2.3 ± 0.2 μm and cell length and width averaged 93.1 ± 5 and 34.6 ± 5.7 μm, respectively (means ± SE, $n = 5$).

Typical force curve and analysis of FN-VSMC adhesion force. To measure the adhesion force between FN and cell surface integrins, FN-coated probes were applied to the surface of VSMC at randomly selected locations between the nucleus and cell margin. Two typical force curves are shown in Fig. 2. The left pointing arrow (blue trace) depicts the approach curve with the force plotted as a function of probe position. As the probe approaches the cell (from *point 1* to *point 2*), force remains at zero level. At the point the probe contacts the cell surface (*point 2*), a resistance is encountered and a force increase is observed. As indentation depth increases, the resistance force increases (*point 2* to *point 3*) until the probe stops approaching and begins to retract. As the probe retraction occurs (right pointing arrow; red trace), the resistance force declines (*point 3* to *point 4*). When there is no adhesion between FN and VSMC, the retraction curve resembles the approach curve (Fig. 2*A*). In contrast, if there were adhesions between the FN-coated AFM probe and the VSMC surface, pulling forces corresponding to the adhesion strength are observed and cantilever deflection is reversed. Abrupt shifts (*point 5*) in the retraction curve (Fig. 2*B*, red trace) occur as adhesions between the probe and cell rupture. When all adhesions between the AFM probe and VSMC have been broken, the retraction curve again resembles the approach curve (Fig. 2*B*, *point 6*).

To analyze the distribution of adhesion events, the observed adhesion forces and corresponding number of events were plotted as histograms (Fig. 2*C*). The bar at the right margin of the histogram shows the probability of FN-VSMC adhesion events. In control experiments, the probability of adhesion between the FN-coated probe and the VSMC was dependent on the concentration of FN coating the AFM probe. For example, with a probe coated with 1 mg/ml FN, the probability of adhesion was 75% (Fig. 2*C*). When the FN coating concentration was reduced to 0.25 mg/ml, the probability of adhesion was decreased to 29%. The adhesion force represented by the initial primary peak was 39 ± 8 pN, and it was not affected by the FN coating concentration. Experiments performed with AFM probes coated with BSA as a nonspecific ligand exhibited a binding probability of only 4% compared with the higher binding probabilities observed with the FN.

FN selectively binds $\alpha_5\beta_1$-integrin on VSMC. To test the binding specificity of adhesion events, function-blocking integrin antibodies were used to block specific FN-integrin bindings. Application of an anti-β_1-integrin antibody (16 μg/ml) significantly reduced the overall probability of FN-VSMC adhesion from 75% to 48%. This antibody had no significant

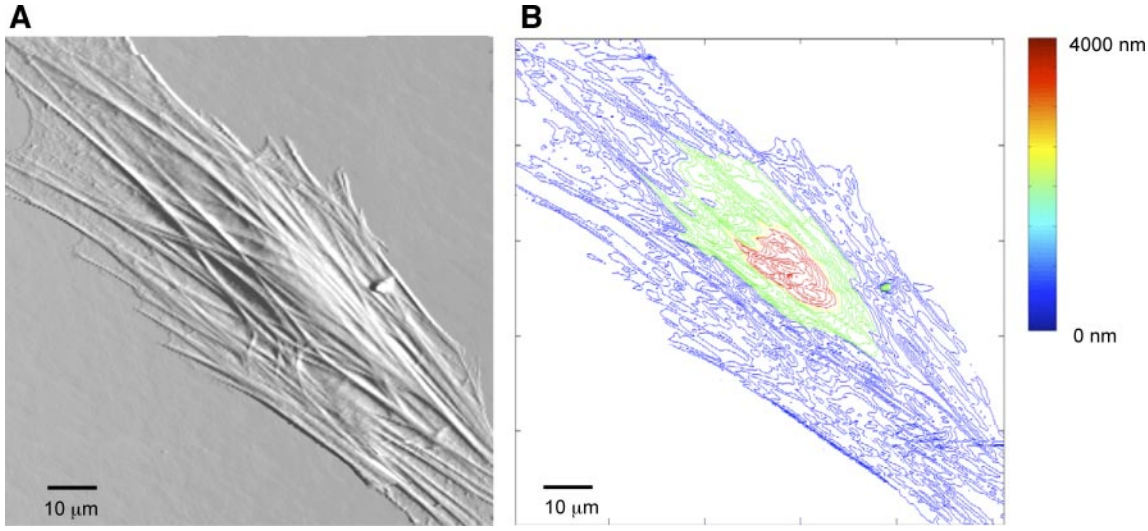

Fig. 1. Deflection image (*A*) and topographic image (*B*) of a cultured vascular smooth muscle cell (VSMC). The image was acquired in cell culture medium at room temperature using contact mode operation of atomic force microscopy (AFM). The AFM probe was scanned across the cell surface at a speed of 40 μm/s, with a tracking deflection force of ~400 pN. Topographic image was generated using the AFM height data. Scale bar represents 10 μm.

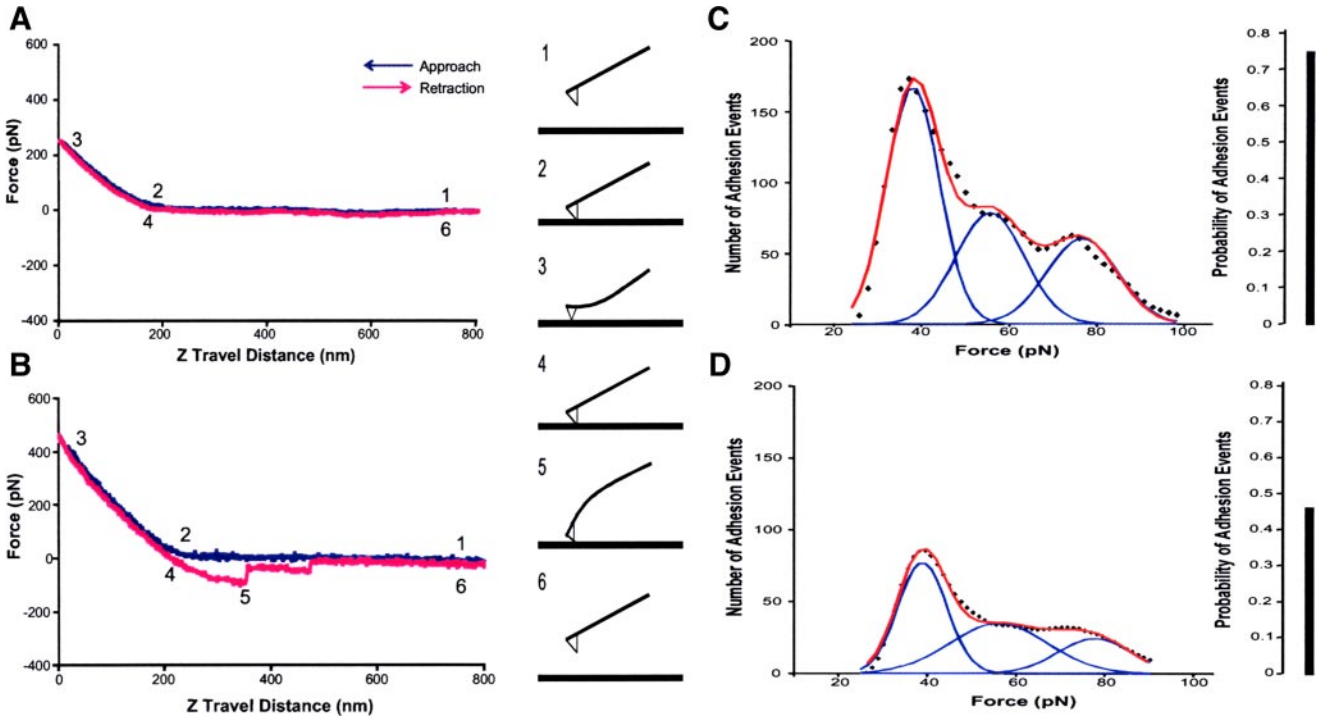

Fig. 2. Typical nonadhesion (*A*) and adhesion (*B*) force curves generated by using AFM. A schematic of the AFM probe movement during the process of force curve generation is shown at center. AFM fibronectin (FN)-coated probes were controlled to repeatedly contact and retract from VSMC surface at a speed of 800 nm/s and 0.5-Hz frequency. During retraction, when a specific adhesion occurred, the rupture of this adhesion was detected as a sharp deflection shift in the retraction curve (*B*). *C* and *D*: force-adhesion events distributions (♦) and integrin-FN binding probabilities (black bar) of control cells (*C*) and cells blocked with a function-blocking antibody against β_1-integrin (*D*). The force-adhesion events distributions were plotted in histograms and were fitted with multiple Gaussian distributions (blue lines). Red lines represent the fitted model of distributions of adhesion events. The binding probability was determined as (number of force curves with adhesions)/(number of total force curves sampled).

effect on the location of the primary force peak but significantly reduced the number of adhesion events (Fig. 2*D*). Increasing the concentration of the anti-β_1-integrin antibody from 16 to 100 μg/ml further reduced the binding probability to 27%. The frequency of events underlying the primary peak (~39 pN) was significantly reduced by the addition of anti-β1 antibody, indicating selective interference with the binding between FN and integrins with β_1-subunit.

The FN-VSMC adhesion was also significantly reduced by a function-blocking anti-α_5-integrin antibody. Blockade of α_5-integrin reduced the binding probability of FN to the cell surface in a concentration-dependent manner. At 16 μg/ml, anti-α_5 reduced the binding probability by 38%, whereas a higher concentration of the antibody (100 μg/ml) reduced the binding probability by 70% (Fig. 3). No inhibition was observed with blocking antibodies against α_4- and β_3-integrins (Fig. 3). In addition, an integrin-binding RGD-containing peptide also reduced the FN-VSMC adhesion in a concentration-dependent manner, whereas an RGE-containing peptide used as control had no effect (Fig. 3). Similar to HMβ1–1 antibody, the HMα5–1 antibody and RGD-containing peptide had no significant effect on the location of the primary force peak (Table 1) but significantly reduced the frequency (height of the peak), indicating that only the probability of FN-$\alpha_5\beta_1$ binding was altered. Collectively, these results indicated that the FN-coated probe selectively bound $\alpha_5\beta_1$-integrins on VSMC and that the interaction was RGD dependent. Thus the observed forces were interpreted to represent the unbinding force of FN-$\alpha_5\beta_1$ bonds.

Immunofluorescence confocal microscopy revealed that $\alpha_5\beta_1$ (in red) was diffusely distributed on the apical surface of VSMC (Fig. 4*A*), with discrete clusters of $\alpha_5\beta_1$ observed at the cell-substrate interface presumably at areas representing focal contacts (Fig. 4*B*). When an FN-coated bead was placed on cell surface, α_5-integrins were observed to form a ringlike cluster around the circumference of the bead (Fig. 4, *C* and *D*).

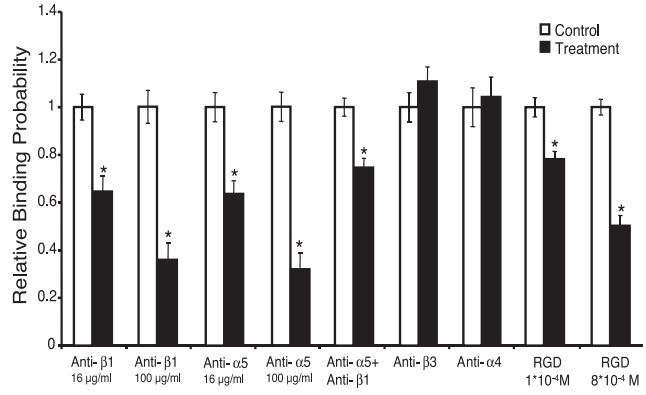

Fig. 3. Relative binding probabilities ± SE of integrin and FN for control VSMC (open bars) and cells blocked with different function-blocking antibodies or RGD-containing peptides (solid bars). For antibody blocking, cells were incubated with specific monoclonal antibodies for 45 min at 37°C before force measurement. A comparable amount of PBS was added to the control cultures. For peptide blocking, cells were incubated with RGD-containing peptide for 45 min at 37°C before force measurement, and control cells were incubated with comparable amount of RGE-containing peptide in the same conditions. $^*P < 0.05$ vs. control.

Table 1. *Unbinding force of FN-$\alpha_5\beta_1$ integrin interaction on VSMC with different treatments*

	Cell Culture Medium (10% Fetal Bovine Serum)						
						RGD	
	Anti-β_1	Anti-α_5	Anti-α_5 + anti-β_1	Anti-β_3	Anti-α_4	1×10^{-4} M	8×10^{-4} M
Control	39	34	39	43	41	37	39
Treatment	39	34	38	42	40	36	39

	Short-Term (2 h) Serum Free			
	PDGF (10 ng/ml)	PDGF (100 ng/ml)	LPA	S1P
Control	38	40	41	39
Treatment	39	41	40	42

	Long-Term (20 h) Serum Free		
	PDGF (100 ng/ml)	LPA	S1P
Control	38	39	39
Treatment	40	39	39

Values are the forces (in pN) of primary peaks in force-adhesion event distributions. Mean of all values shown is 39 pN. Because the spring constant calibration bears a 20% error, the estimated bond strength of $\alpha_5\beta_1$-fibronectin (FN) is 39 ± 8 pN. VSMC, vascular smooth muscle cell; PDGF, platelet-derived growth factor; LPA, lysophosphatidic acid; S1P, sphingosine-1-phosphate.

Regulation of $\alpha_5\beta_1$-FN binding probability. The effects of serum starvation on FN-$\alpha_5\beta_1$ interaction were investigated. After serum starvation for 2 or 20 h, significant decreases (40%) in FN-VSMC adhesion probability were observed compared with cells maintained in serum-containing media (Fig. 5*A*). However, there was no significant change in the FN-$\alpha_5\beta_1$ unbinding force (39 vs. 39 pN, 2-h serum starvation; and 43 vs. 42 pN, 20-h serum starvation, respectively). To determine if the decreased FN-integrin adhesion was induced by changes in the ability of the integrins to functionally bind FN or by changes in the protein expression of $\alpha_5\beta_1$ on the cell, VSMC were examined by flow cytometry. As shown in Fig. 5*B*, cell membrane expression of $\alpha_5\beta_1$ was not changed after 2 h of serum starvation but was significantly decreased (70%) after 20 h of serum starvation. Taken together, these data indicate that 2-h serum starvation decreased FN-$\alpha_5\beta_1$ adhesion by mechanisms other than altering the cell membrane protein expression of $\alpha_5\beta_1$. In contrast, after 20-h serum starvation, a reduced cell membrane expression of $\alpha_5\beta_1$ was observed that could contribute to the decrease in FN-$\alpha_5\beta_1$ adhesion (Fig. 5*B*).

To identify possible serum-containing molecules that might be regulating the FN-$\alpha_5\beta_1$ interaction, we tested the effect of three serum-derived molecules: PDGF-BB (10 ng/ml and 100 ng/ml), S1P (1 μM), and LPA (1 μM), on the binding probability and unbinding force of FN-$\alpha_5\beta_1$ bond. When VSMC were subjected to 2-h serum starvation, PDGF further reduced the probability of FN-$\alpha_5\beta_1$ binding in a concentration-dependent manner (Fig. 6*A*). In contrast, LPA (1 μM) significantly enhanced the probability of $\alpha_5\beta_1$ binding to FN. S1P had no significant effect on FN binding probability. PDGF also reduced the probability of $\alpha_5\beta_1$ binding to FN after 20-h serum starvation, whereas both LPA and S1P had no apparent effects (Fig. 6*B*). None of the treatments had a significant effect on the primary force peak used as estimation of unbinding force (Table 1). The effects of LPA and PDGF on the surface expression of $\alpha_5\beta_1$-integrin were also examined by flow cytometry. As shown in Fig. 7, 2-h treatment with LPA and PDGF had no significant effect on the surface expression of $\alpha_5\beta_1$ in either short- or long-term serum-starved cells. We also examined the effect of LPA and PDGF on integrin distribution with confocal fluorescence microscopy and found no significant change compared with control images (data not shown).

Because integrin binding and cluster formation is a time-dependent process, we sought to determine whether the rate of adhesion to an FN-coated bead was altered by serum, PDGF-BB, or LPA. A series of experiments were performed in which an AFM probe with an FN-coated bead (2-μm diameter) was allowed to contact the surface of the VSMC for increasing lengths of time (2, 5, and 8 min). In control cells, the force required to detach the FN-coated bead from the cell surface increased as the duration of contact time increased (Fig. 8*A*). Treatment of the cells with LPA shifted the force vs. time relationship upward without changing the slope of the relationship (Fig. 8*A*). In contrast, treatment with PDGF-BB caused a downward shift in the force vs. time relationship as well as a decrease in the slope of the relationship. The downward-shifted PDGF-BB curve also exhibited a plateau (Fig. 8*A*). Treatment of the cells with serum produced an upward shift in the relationship that was nonlinear with the curves being parallel up to 5 min, and beyond that the serum-treated cells exhibited an apparent plateau (Fig. 8*B*).

DISCUSSION

In this study, we demonstrate that AFM can be used to selectively investigate the mechanical characteristics of the initial interactions between FN and $\alpha_5\beta_1$ on rat VSMC. These initial adhesive interactions are postulated to precede the integrin clustering events and ultimate assembly of a mature focal contact. With respect to the focal contact, it has been hypothesized that it is the collective recruitment at the site of the initial adhesion of cytoskeletal proteins and downstream signaling proteins that provides a pathway for mechanosensation and transmission of forces (e.g., 12). Careful analysis of the initial adhesions and their unbinding forces indicated that the

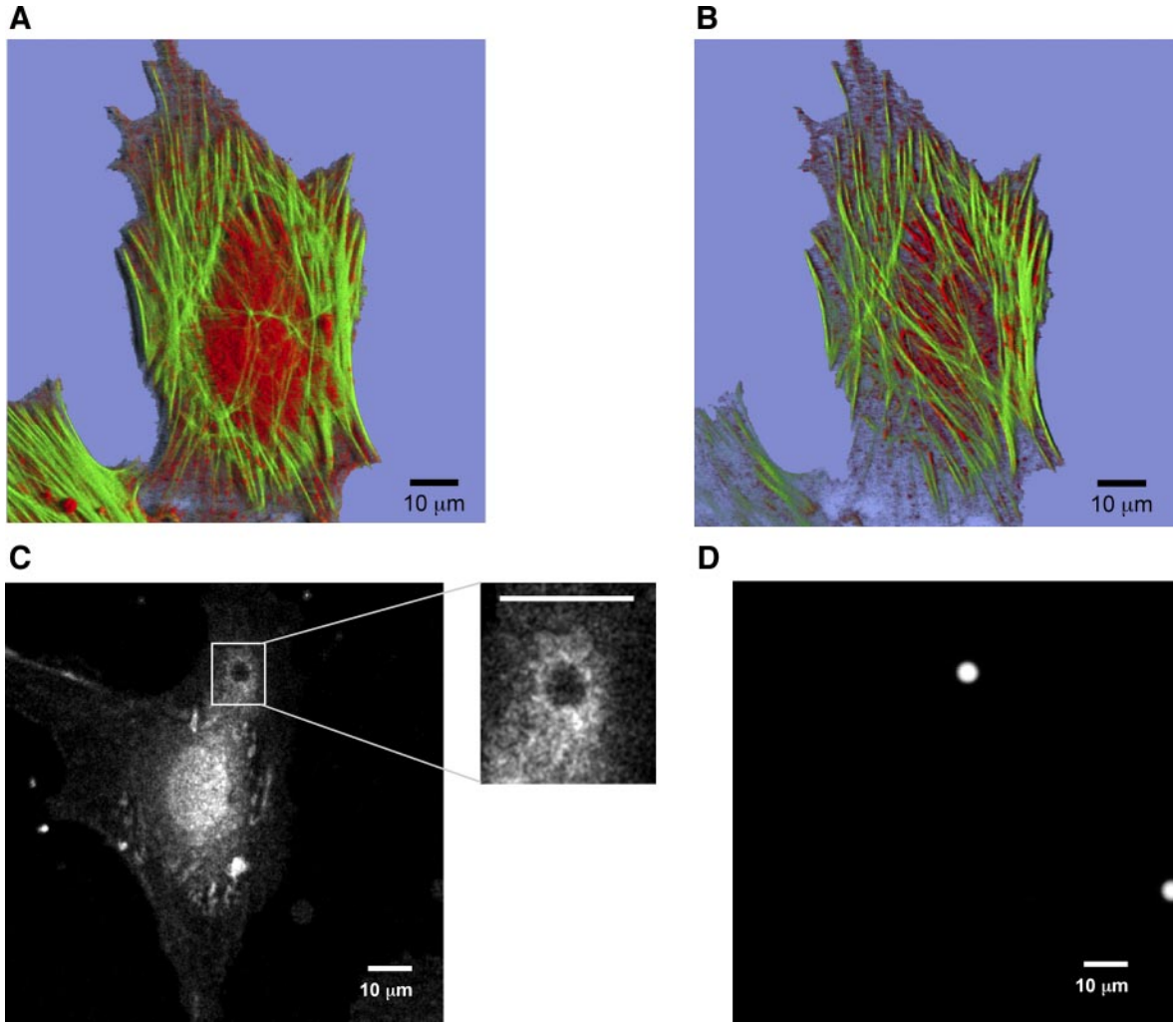

Fig. 4. The distribution of $\alpha_5\beta_1$-integrins on VSMC. Cells were immunofluorescently labeled with antibodies against $\alpha_5\beta_1$-integrin (red) and with phalloidin against actin filaments (green). A through-focus image set was collected for the cell with a *z*-step interval of 0.2 μm. The confocal images were processed using Imaris software (Bitplane, Zurich, Switzerland). *A*: top view of a reconstructed 3-dimensional image of a smooth muscle cell. $\alpha_5\beta_1$-Integrin is clearly present on cell surface in a diffusive pattern. *B*: bottom view of the same smooth muscle cell (3-dimensional reconstruction of a stack of cell bottom confocal images), where integrin clusters occur along the actin filaments. *C*: confocal image showing FN-coated bead (5-μm diameter) caused $\alpha_5\beta_1$-integrin clustering on the apical surface of the SMC cell. *Inset*: amplified image of the bead induced integrin clustering. *D*: confocal image of the bead (labeled with dragon green) on top of the cell shown in *C*. Scale bars represent 10 μm.

force required to rupture the bond between $\alpha_5\beta_1$ and FN was 39 ± 8 pN. Serum starvation, as well as PDGF-BB and LPA, was found to modulate the FN-$\alpha_5\beta_1$ binding probability but not the estimated unbinding force. These factors also modulated the rate of formation of a focal contact with an FN-coated bead. Collectively, our results suggest that binding between FN and $\alpha_5\beta_1$ and the formation of focal contacts in VSMC is strongly influenced by factors that alter the binding activity of $\alpha_5\beta_1$.

That the interactions between the FN-coated AFM probe and the surface of VSMC involved $\alpha_5\beta_1$-integrin is supported by a number of observations. First, the reduction in adhesion probability observed in the presence of anti-α_5 and anti-β_1 function-blocking antibodies indicated this integrin was involved in mediating adhesion. It was observed that combining anti-α_5 and anti-β_1 function-blocking antibodies did not have an additive effect, which would be consistent with the ability of both antibodies to target the same receptor and to effectively block that receptor without an interaction. Furthermore, soluble RGD-containing peptides reduced, while anti-β_3 and anti-α_4 function-blocking antibodies did not affect, the adhesion. Thus these observations indicate that the FN-coated AFM probe was interacting with $\alpha_5\beta_1$ in an RGD-dependent manner.

In accordance with Benoit et al. (4), we used the initial or primary force peak in the force-frequency distribution to determine the adhesion force of a single FN-$\alpha_5\beta_1$ bond. Based on Poisson statistics, when binding probability is <20%, 90% of the observed binding events should originate from single pair of protein interactions, such that a discrete peak in the low force range of the force-frequency plot represents the adhesion or binding force of a single pair of protein bindings (4). In all of the experiments conducted, we observed that a discrete histogram peak occurred at 34–43 pN that was not significantly affected by any of the treatments. Although higher unbinding forces were characteristic of subsequent peaks in the force-frequency distribution, their interpretation is less certain. They could represent multiple bonds that rupture simulta-

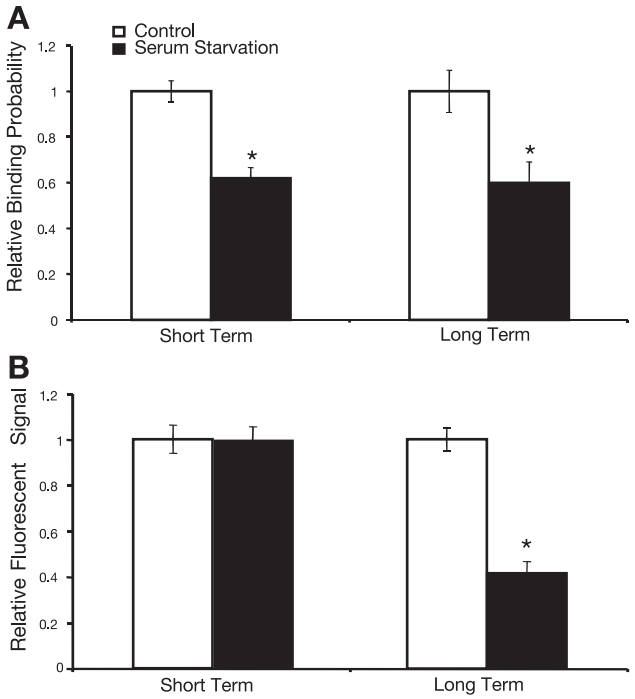

Fig. 5. *A*: relative binding probabilities ± SE of integrin and FN in control VSMC (open bar) and serum-starved cells (solid bar). *$P < 0.05$ vs. control. *B*: cell membrane expression of $\alpha_5\beta_1$-integrin in control cells (open bar) and serum-starved cells (solid bar). Cell membrane expression of $\alpha_5\beta_1$ was determined using flow cytometry. The median of the fluorescent signal was used to represent the average level of $\alpha_5\beta_1$-integrin. Experiments were conducted in triplicate. For serum starvation, cells were incubated in DMEM/F-12 medium without serum for 2 h (short-term serum starvation) or for 20 h (long-term serum starvation) at 37°C. *P <0.05 vs. control.

neously, populations of the receptor that bind more tightly, differences in the FN-binding conformation on the AFM probe tip, differences in the manner in which different integrins are tethered to the cell, or local variation in loading rate. Despite the inability to clearly interpret what these forces represent, the ability of function-blocking antibodies to α_5 and β_1, reduced FN tip concentration, and RGD peptide to decrease adhesion events at these higher forces support involvement of the FN-$\alpha_5\beta_1$ interaction. Higher forces have also been reported by Lehenkari and Horton (13). They determined that the adhesion forces ranged from 32 to 97 pN for integrin bindings with several ECM proteins and RGD-containing peptides on osteoclasts (13). Li and colleagues (14) also measured the $\alpha_5\beta_1$-integrin-FN adhesion force on K562 cells using AFM and reported that the adhesion force varied depending on the force-loading rate and could range from 40 to 140 pN (14). Thus there is overall close agreement concerning the scale of forces required to rupture the bond between integrins and ECM proteins.

We also considered the possibility that some of the forces measured in our study may represent events other than the rupture of the FN-$\alpha_5\beta_1$ bond. These events include the possibility of pulling integrins from the cell membrane, the unfolding of FN on the AFM tip, and/or the detachment of FN from the probe. In this regard, all of these possibilities have been reported by others to require forces that exceed our estimated force for a single FN-$\alpha_5\beta_1$-integrin bond. Shao and Hochmuth (21) found that removing β_2-integrins from neutrophil membranes required a force of 60–130 pN applied over 1–4 s (21). Rief et al. (20) estimated the unfolding force of bovine plasma fibronectin to be 60~130 pN and observed that force curves followed a sawtooth pattern with peak spacings of $\Delta L = 30$ nm (20). It is clear from our force curve that the sawtooth unfolding pattern did not occur and that the scale of the unfolding forces is larger than the single-bond strength detected in our experiment. In control experiments, we also tested the force required to detach FN from the AFM tips and that forces that were in excess of ~300 pN were required. Unbinding forces have also been shown by others to depend on loading rate, with larger forces measured at higher loading rate (14, 18), thus raising the possibility that some of the splay in the observed histograms and perhaps the higher forces could be related to local variations in loading rate. Other possible influences on the measured forces include binding to a heterogeneous population of receptors, nonspecific binding of FN to the cell, and changes in cell properties such as membrane fluidity that could result in altered integrin mobility. These factors could contribute to the observed secondary peaks and splay in the distribution of forces. Taken together, we have interpreted the initial peak in the binding force measurements to be a faithful representation of the force required to detach FN from $\alpha_5\beta_1$.

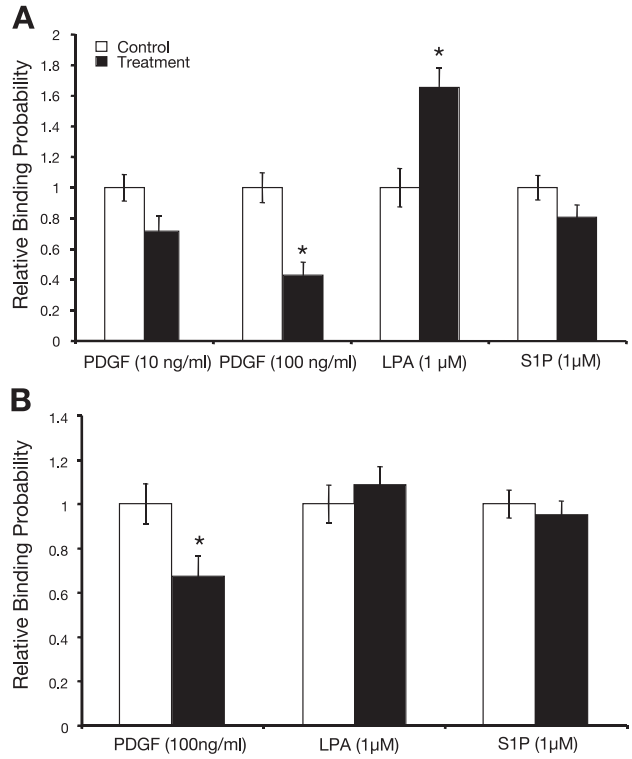

Fig. 6. *A*: relative binding probabilities ± SE of $\alpha_5\beta_1$ and FN in VSMC serum-starved for 2 h (open bar) and cells serum-starved in the presence of lysophosphatatic acid (LPA), platelet-derived growth factor (PDGF), or sphingosine-1-phosphate (S1P) (solid bars). LPA, S1P, and PDGF-BB were added into cell culture immediately after cells were incubated in serum-free medium. Cells were incubated with/without these factors at 37°C for 2 h before adhesion force measurement. *$P < 0.05$ vs. control. *B*: relative binding probabilities ± SE of integrin and FN in VSMC serum starved for 20 h (open bar) and cells incubated with LPA, PDGF, or S1P and 20 h of serum starvation (solid bar). Cells were incubated in serum-free medium at 37°C for 18 h before LPA, S1P, or PDGF-BB were added into the medium. Cells were incubated with these molecules for another 2 h before the measurement of adhesion force. *$P <$ 0.05 vs. control.

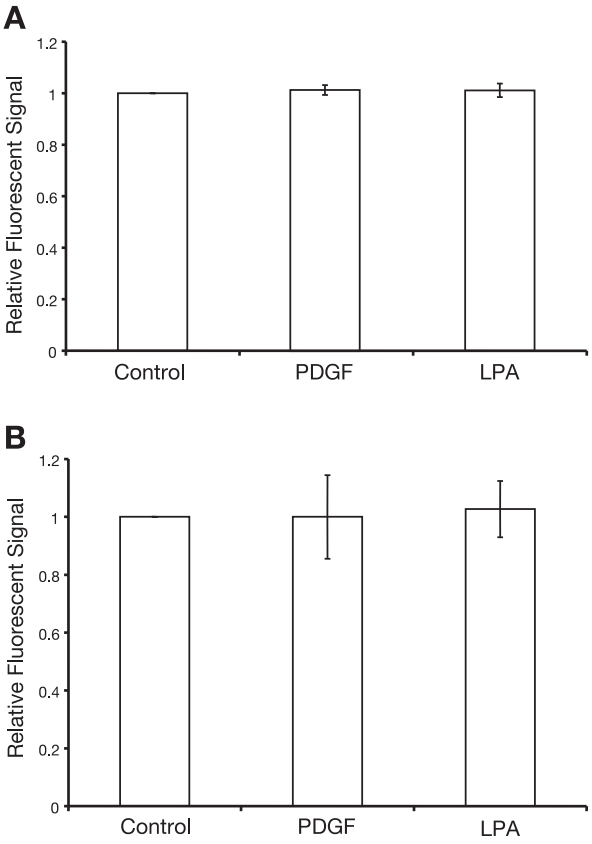

Fig. 7. Lack of effect of LPA and PDGF treatment on cell membrane expression of $\alpha_5\beta_1$ as determined using flow cytometry. The median of fluorescent intensity was used to estimate the average level of $\alpha_5\beta_1$ expression. Two experiments were combined with each conducted in triplicate. *A*: short-term serum starvation. VSMC serum-starved for 2 h (control) and cells serum-starved in the presence of LPA or PDGF for 2 h. *B*: long-term serum starvation. VSMC serum-starved for 20 h (control) and cells treated with LPA and PDGF after 20 h of serum starvation. Cells were incubated in serum-free medium for 18 h before being treated with LPA and PDGF-BB for another 2 h.

A number of experiments were performed to determine if serum or serum-containing factors would alter the mechanical characteristics of the FN-$\alpha_5\beta_1$ interaction. Specifically, we sought to determine whether binding probability and/or the unbinding force were altered. In this regard, FN-$\alpha_5\beta_1$ binding probability decreased by 40% after both short-term (2 h) and long-term serum starvation (20 h). However, a change in the estimated unbinding force was not observed under any of the experimental conditions. Further studies showed that only long-term serum starvation decreased the cell membrane expression of $\alpha_5\beta_1$, whereas short-term serum starvation had no apparent effect on cell membrane expression of the integrin. Fluorescence immunocytochemistry confirmed that after 2 or 20 h of serum starvation the overall spatial distribution of $\alpha_5\beta_1$ on VSMC was similar to cells with serum (data not shown). In summary, these observations suggested that serum-derived factors were altering FN-$\alpha_5\beta_1$ binding probability in part by changing expression level on VSMC as seen in the 20 h serum-starved cells and by other mechanisms affecting the ability of $\alpha_5\beta_1$ to bind FN as seen in the 2-h serum-starved cells.

Our results indicate that a serum-derived factor that does affect the FN-$\alpha_5\beta_1$ interaction is PDGF-BB. FN-$\alpha_5\beta_1$ binding was reduced by PDGF-BB after both short- and long-term serum starvation (Fig. 6). The reduction in binding probability in the presence of PDGF-BB argues against its playing a role in reducing binding on withdrawal of serum. In other work, Berrou and Bryckaert (5) reported that short-term (1 h) treatment of pig aorta smooth muscle cells with PDGF-BB reduced cell adhesion to FN through $\alpha_5\beta_1$-integrin, which is consistent with our results. PDGF has long been recognized as a potent stimulator for VSMC proliferation and migration. In the balloon-injured baboon artery, the integrin β_1 expression and the active integrin β_1 forms were both found decreased in neointimal VSMC (11). Because PDGF is one of the major growth factors released during arterial injury, our study may provide a possible mechanism for the reduced activity of this integrin and its interactions with FN.

In contrast to PDGF-BB, LPA enhanced FN-$\alpha_5\beta_1$ binding probability after short-term serum starvation whereas no enhancement was found after long-term serum starvation. Similar to PDGF-BB, LPA had no effect on the measured unbinding

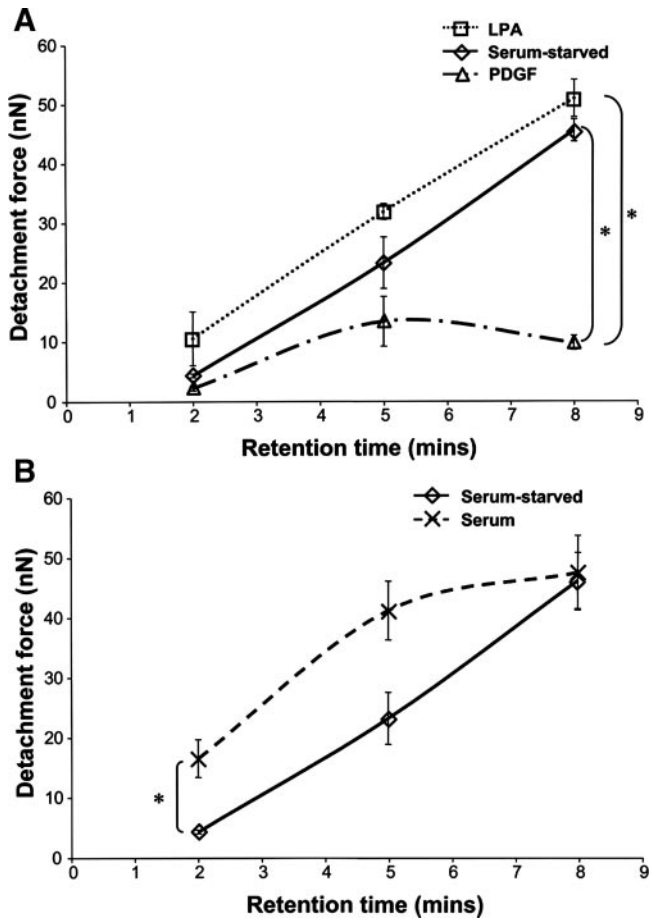

Fig. 8. Detachment force as a function of the contact time of FN-coated beads applied to the cell surface. The FN-coated beads were fused with AFM cantilever and were put into contact with cell surface for increasing periods of contact with the cell (2, 5, and 8 min). The beads were then lifted from the cell using the AFM to measure the detachment force. *A*: effect of LPA and PDGF. VSMC were serum-starved for 2 h (◇, solid line, $n = 14$) or serum-starved in the presence of LPA (1 μM) (□, dotted line, $n = 15$) or PDGF (100 ng/ml) (△, dash-dotted line, $n = 23$). *B*: comparison between short-term serum-starved VSMC (◇, solid line) and nonstarved VSMC (×, dashed line, $n = 20$). *$P < 0.05$.

forces. The ability of LPA to increase adhesive interactions between FN and $\alpha_5\beta_1$ make it a possible candidate that can account for the effects observed with serum starvation. The lack of effect of LPA on FN binding in the long-term serum-starved cells suggests that the pool of available integrin receptors is refractory to its effects. This might be expected if the majority of the integrins that are expressed on the cell surface are active and available for binding.

Various possibilities to explain the effects of serum withdrawal, PDGF-BB, and LPA on binding probability were considered. One possibility is that there was a change in integrin mobility within the cell membrane. For example, if integrins became more freely or rapidly diffusible within the membrane, then an increased probability of binding would be anticipated. Additionally, regulatory events that alter an integrin's ability to bind its ligand could play a role in modulating binding probability because this would alter the size of the available pool of integrins for binding. As such, integrin activation would be anticipated to increase the binding probability, whereas inactivation would reduce binding probability. Regardless of the precise mechanism, the data clearly show that $\alpha_5\beta_1$ interactions with FN can be rapidly modulated in vascular smooth muscle.

Although serum starvation, PDGF, and LPA had significant effects on binding probability, these treatments did not significantly change the FN-$\alpha_5\beta_1$ characteristic unbinding force. Similarly, Litvinov et al. (15) have also shown that the rupture force of $\alpha_{IIb}\beta_3$-fibrinogen was not affected by platelet-activating factors. However, it has to be noted that the AFM system has limitations in detecting small force differences because calibration of the spring constant carries a measurement error of ~20%. Thus it is not possible to rule out that small shifts of the FN-$\alpha_5\beta_1$ unbinding force undetectable by the AFM system may have occurred and gone undetected. As such, the reported bond strength measurements may not reflect an integrin affinity change. There is also evidence to suggest that the binding between FN and $\alpha_5\beta_1$ might involve a multistep process leading to the final binding state, which determines the mature bond strength, and this could be different from the initial engagement state, that is subject to integrin affinity regulation (9). Despite our lack of evidence for a change in bond strength, the observed changes in binding probability demonstrate clearly that there are other mechanisms that can rapidly regulate the binding activity of $\alpha_5\beta_1$.

To gain additional mechanistic insight into the effects of serum removal, PDGF-BB, and LPA, experiments were performed with FN-coated beads to increase the number of integrin-FN interactions and examine how those interactions changed over time. The experiments performed showed that the force required to detach the bead from the cell increased as a function of the bead's residence time on the surface of the cell. This is consistent with a process that increases the strength of mechanical linkage between cell and bead. An observed accumulation of α_5 beneath FN-coated beads was also observed in our study. Thus events involving integrin clustering and focal adhesion formation with cytoskeletal participation would be consistent with these observations (6). In fibroblasts, laser-trapped beads coated with FN stiffen with increasing length of contact with the cell (7). Lammerding et al. (12) also reported adhesion strengthening over time mediated by $\alpha_6\beta_1$-integrin and laminin (12). Similarly, tensional forces applied to magnetic beads that are coated with RGD-containing peptide or anti-integrin antibodies demonstrated strengthening of the focal adhesion between bead and cell as a function of focal adhesion assembly (17). Thus the bead experiments provide a mechanical means for evaluating not only the interaction between FN and $\alpha_5\beta_1$ but also events related to assembly of the focal contact and cytoskeleton beneath the adhesion site.

Using the detachment strength as a function of time as our experimental model, we reasoned that a change in the slope of the relationship would be indicative of a change in the rate of integrin attachment and/or focal adhesion assembly. Furthermore, we reasoned that a change in intercept would likely reflect changes in the apparent density of integrins on the cell surface that were available for binding. Treatment of cells with LPA did not cause any significant changes in the slope of the force vs. time relationship. However, LPA and serum treatment caused an upward shift of the relationship so that at any given time more force was required to detach the bead. These observations suggest that the number of integrins available for binding was increased but the rate at which the attachment was strengthened was unaltered. The observed plateau seen with serum treatment may indicate that the number of receptors available for binding was becoming saturated. An increased number of integrins available for binding would be consistent with the increased binding probability we observed between FN and the cell surface after LPA treatment. In contrast, treatment with PDGF-BB caused a downward shift of the relationship and a decrease in the slope. This is also consistent with our binding probability data as a downward shift in the relationship would be associated with a decreased binding probability. However, the decreased slope of the relationship and plateau also suggests that PDGF-BB negatively affected the rate of the process involved in integrin clustering and/or focal adhesion development.

GRANTS

This work was supported by National Heart, Lung, and Blood Institute Grants HL-58960 and HL-062863 to G. A. Meininger.

REFERENCES

1. **Alberts B, Bray D, Lewis J, Raff M, Roberts K, and Watson JD.** *Molecular Biology of the Cell (*3rd ed.). New York: Garland, 1994, p. 857.
2. **Allen S, Davies J, Davies MC, Dawkes AC, Roberts CJ, Tendler SJ, and Williams PM.** The influence of epitope availability on atomic-force microscope studies of antigen-antibody interactions. *Biochem J* 341: 173–178, 1999.
3. **Bayless KJ and Davis GE.** Sphingosine-1-phosphate markedly induces matrix metalloproteinase and integrin-dependent human endothelial cell invasion and lumen formation in three-dimensional collagen and fibrin matrices. *Biochem Biophys Res Commun* 312: 903–913, 2003.
4. **Benoit M, Gabriel D, Gerisch G, and Gaub HE.** Discrete interactions in cell adhesion measured by single-molecule force spectroscopy. *Nat Cell Biol* 2: 313–317., 2000.
5. **Berrou E and Bryckaert M.** Platelet-derived growth factor inhibits smooth muscle cell adhesion to fibronectin by ERK-dependent and ERK-independent pathways. *J Biol Chem* 276: 39303–39309, 2001.
6. **Burridge K and Chrzanowska-Wodnicka M.** Focal adhesions, contractility, and signaling. *Annu Rev Cell Dev Biol* 12: 463–518, 1996.
7. **Choquet D, Felsenfeld DP, and Sheetz MP.** Extracellular matrix rigidity causes strengthening of integrin-cytoskeleton linkages. *Cell* 88: 39–48, 1997.
8. **Davis MJ, Wu X, Nurkiewicz TR, Kawasaki J, Davis GE, Hill MA, and Meininger GA.** Integrins and mechanotransduction of the vascular myogenic response. *Am J Physiol Heart Circ Physiol* 280: H1427–H1433, 2001.

9. **Garcia AJ, Schwarzbauer JE, and Boettiger D.** Distinct activation states of α5β1 integrin show differential binding to RGD and synergy domains of fibronectin. *Biochemistry* 41: 9063–9069, 2002.
10. **Hughes PE and Pfaff M.** Integrin affinity modulation. *Trends Cell Biol* 8: 359–364, 1998.
11. **Koyama N, Seki J, Vergel S, Mattsson EJ, Yednock T, Kovach NL, Harlan JM, and Clowes AW.** Regulation and function of an activation-dependent epitope of the β1 integrins in vascular cells after balloon injury in baboon arteries and in vitro. *Am J Pathol* 148: 749–761, 1996.
12. **Lammerding J, Kazarov AR, Huang H, Lee RT, and Hemler ME.** Tetraspanin CD151 regulates α6β1 integrin adhesion strengthening. *Proc Natl Acad Sci USA* 100: 7616–7621, 2003.
13. **Lehenkari PP and Horton MA.** Single integrin molecule adhesion forces in intact cells measured by atomic force microscopy. *Biochem Biophys Res Commun* 259: 645–650, 1999.
14. **Li F, Redick SD, Erickson HP, and Moy VT.** Force measurements of the α5β1 integrin-fibronectin interaction. *Biophys J* 84: 1252–1262, 2003.
15. **Litvinov RI, Shuman H, Bennett JS, and Weisel JW.** Binding strength and activation state of single fibrinogen-integrin pairs on living cells. *Proc Natl Acad Sci USA* 99: 7426–7431, 2002.
16. **Martinez-Lemus LA, Wu X, Wilson E, Hill MA, Davis GE, Davis MJ, and Meininger GA.** Integrins as unique receptors for vascular control. *J Vasc Res* 40: 211–233, 2003.
17. **Matthews BD, Overby DR, Alenghat FJ, Karavitis J, Numaguchi Y, Allen PG, and Ingber DE.** Mechanical properties of individual focal adhesions probed with a magnetic microneedle. *Biochem Biophys Res Commun* 313: 758–764, 2004.
18. **Merkel R, Nassoy P, Leung A, Ritchie K, and Evans E.** Energy landscapes of receptor-ligand bonds explored with dynamic force spectroscopy. *Nature* 397: 50–53, 1999.
19. **Moy VT, Florin EL, and Gaub HE.** Intermolecular forces and energies between ligands and receptors. *Science* 266: 257–259, 1994.
20. **Rief M, Gautel M, and Gaub HE.** Unfolding forces of titin and fibronectin domains directly measured by AFM. *Adv Exp Med Biol* 481: 129–136, 2000.
21. **Shao JY and Hochmuth RM.** Mechanical anchoring strength of L-selectin, β2 integrins, and CD45 to neutrophil cytoskeleton and membrane. *Biophys J* 77: 587–596, 1999.
22. **Wang N, Butler JP, and Ingber DE.** Mechanotransduction across the cell surface and through the cytoskeleton. *Science* 260: 1124–1127, 1993.
23. **Woodside DG, Liu S, and Ginsberg MH.** Integrin activation. *Thromb Haemost* 86: 316–323, 2001.
24. **Wu X, Mogford JE, Platts SH, Davis GE, Meininger GA, and Davis MJ.** Modulation of calcium current in arteriolar smooth muscle by αvβ3 and α5β1 integrin ligands. *J Cell Biol* 143: 241–252, 1998.